Raman spectroscopic study of $Zr_{1-x}Hf_xW_2O_8$ solid solutions by rapid solid-state reactions

X. Y. GUO, Y. S. ZHANG, C. X. CHENG
Department of Mathematics & Physics, Luoyang Institute of Science and Technology, Luoyang 471023, China

By rapid solid-state reactions, materials with formula $Zr_{1-x}Hf_xW_2O_8$ solid solutions have been successfully synthesized and their structures and phase transitions have been studied. The appropriate temperature and sintering time are 1573 K and 30~60 min, respectively. Compared with traditional Solid Phase Reaction methods，this rapid synthetic method simplifies the production process and reduces the sintering time and energy consumption greatly. Powder XRD and Raman spectroscopic analyses reveal that the $Zr_{1-x}Hf_xW_2O_8$ solid solutions are cubic ZrW_2O_8 type in crystal structure at room temperature. Substitutions using equivalent alter the properties of ZrW_2O_8 such as cell parameters, order-disorder phase transformation temperatures and thermal stability. Temperature dependent Raman spectroscopic studies demonstrate that the order–disorder phase transition temperature increases with increasing the content of Hf and not only the librational motion of the WO_4 tetrahedra and the ZrO_6/HfO_6 octahedra but also the correlated motions of transilation and libration with the asymmetric stretching vibrations of the polyhedra are responsible for the negative thermal expansion in the low-temperature phase.

(Received December 13, 2013; accepted May 7, 2015)

Keywords: Rapid solid-state reaction, Solid solutions, Negative thermal expansion, Raman spectroscopy

1. Introduction

Negative thermal expansion (NTE) materials have been receiving increasing attention for their potential applications in engineering materials with controlled coefficients of thermal expansion (CTE) by compositing them with positive thermal expansion materials [1-8]. Among the NTE materials, ZrW_2O_8 is of considerable interest due to its large isotropic NTE over an extended range of temperature (0.3 ~ 1050 K) [1,2]. Cubic ZrW_2O_8 materials have an open framework structure in which each WO_4 tetrahedron shares three of its four oxygen atoms with adjacent ZrO_6 octahedra and leave one corner linkage free. This framework structure and the libration of the WO_4 and ZrO_6 polyhedral units result in its isotropic negative thermal expansion in a very wide temperature range. It undergoes an order-disorder transformation at about 440 K from its metastable, low-temperature cubic phase (α, space group $P2_13$) with a CTE of ~ -9×10-6 K^{-1} to a metastable, high-temperature cubic phase (β) with a CTE of ~ -5×10-6 K^{-1} [2,4,7,8].

Theoretical studies of the thermal expansion of ZrW_2O_8 were conducted with two methods, geometrical modeling by Rigid Unit Mode (RUM) method and lattice dynamic calculations by free energy minimization (FEM) method or by first principles calculations. The NTE behavior in ZrW_2O_8 is related to the transverse vibration of an O atom in the W-O-Zr linkages and a rigid unit model (RUM) with low energy modes [9,10]. G. Ernst et al [11] have investigated the phonon modes with low energies from 1.5 to 8.5 MeV (12.1– 68.6 cm^{-1} or 17.4–98.6 K) and assumed that those phonons with low energies have equal Grüneisen parameters of -14±2, which are relevant for NTE in ZrW_2O_8.

In this work, a range of $Zr_{1-x}Hf_xW_2O_8$ samples were prepared by the solid state reaction with less time. It is shown that the samples can be synthesized within 60min. The structure changes and properties of $Zr_{1-x}Hf_xW_2O_8$ are studied by X-ray diffraction and Raman spectroscopy. Particular attention has been paid to the Raman spectra at different temperatures of $Zr_{1-x}Hf_xW_2O_8$ in understanding the mechanisms of negative thermal expansion from phonon behaviors by Raman spectroscopic studies. To our knowledge, no Raman spectroscopy on the vibrational properties of $Zr_{1-x}Hf_xW_2O_8$ has been studied so far.

2. Experimental

$Zr_{1-x}Hf_xW_2O_8$ solid solutions were synthesized by the solid state reaction from stoichiometric amounts oxides of ZrO_2 (99.9% pure), HfO_2 (99.9% pure), and WO_3 (99.9% pure). The starting commercial chemicals were mixed according to the stoichiometric ratios of destination materials of $Zr_{1-x}Hf_xW_2O_8$. The mixtures were ground in an agate mortar for 3h, and then pressed into ϕ 6 mm and 15mm thick pellets with a 10MPa pressure. The pellets were then sintered at 1573 K for 30~60 min, and then

quenched quickly in cold water to prevent the solid solutions from decomposition into zirconium oxide and tungsten oxide. All the as-synthesized samples was analyzed by X-ray diffraction (XRD) with a X'Pert PRO X-ray Diffractometer and by Raman spectroscopy with a Renishaw MR-2000. A laser excitation wavelength of 532 nm was used. A TMS 94 heating/freezing stage from Linkam Scientific Instruments Ltd with an accuracy of± 0.1 K was used to record the temperature dependence of the Raman spectra.

3. Results and discussion

3.1 Crystal structure of $Zr_{1-x}Hf_xW_2O_8$ solid solutions

Fig. 1 shows XRD patterns of $Zr_{1-x}Hf_xW_2O_8$ for x =0, 0.3, 0.4, 0.6, 0.7and 0.9; respectively. It can be seen the XRD peaks shifting to bigger angles with the increasing contents of Hf^{4+}, indicating a progressive decrescence of the lattice constants by substitution of Zr^{4+} by Hf^{4+} in ZrW_2O_8. From the facts, we can deduce that (i) All samples of $Zr_{1-x}Hf_xW_2O_8$ solid solutions prepared were characterized to be a single phase having a cubic ZrW_2O_8 type crystal structure (space group $P2_13$) by a powder XRD method. The dependence of the lattice constants on hafnium content follows the Vegard's law, and $Zr_{1-x}Hf_xW_2O_8$ is considered to form a complete solid solution. (ii) The iron radius of Hf^{4+}(85 pm) is smaller than that of Zr^{4+} (86 pm) and it induces the lattice constants of $Zr_{1-x}Hf_xW_2O_8$ (x = 0–1) substituted by the same valence decrease linearly with increasing hafnium content.

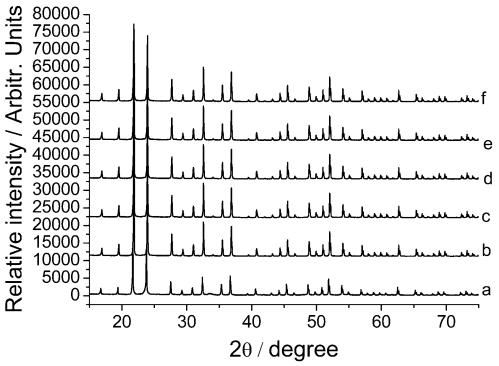

Fig. 1. X-ray diffraction patterns of $Zr_{1-x}Hf_xW_2O_8$: (a) x=0, (b) x=0.3, (c)x=0.4,(d)x=0.6,(e)x=0.7,（f）x=0.9.

3.2 Raman spectroscopic study of $Zr_{1-x}Hf_xW_2O_8$ solid solutions

HfW_2O_8 having a Hf^{4+} cation at the center of octahedral has the same crystal structure as ZrW_2O_8, and shows the negative thermal expansion similarly to ZrW_2O_8. The cubic phase of HfW_2O_8 has four formula units per unit cell. This results in 44 atoms in the unit cell and consequently a total of 132 degrees of freedom, which manifest themselves as acoustic and optic phonons. According to factor group analysis, all the 54 optical phonon modes of HfW_2O_8 are Raman active.

Fig. 2 shows the Raman spectra of $Zr_{1-x}Hf_xW_2O_8$ solid solutions at room temperature. The frequencies for a free tungstate ion are close to 930, 830, 405 and 320 cm^{-1}. By comparison with Raman spectra of the free tungstate ion, the Raman modes from 1040 to 910 cm^{-1}, from 910 to 700 cm^{-1}, from 400 to 320 cm^{-1}, from 320 to 280 cm^{-1} were previously identified as symmetric stretching (ν_1), asymmetric stretching (ν_3), symmetric bending (ν_4), asymmetric bending (ν_2) modes in the WO_4 tetrahedra in α-ZrW_2O_8. The other modes below 280 cm^{-1} were ascribed to the lattice modes arising from Zr atom motions and translational and librational motions of the WO_4 tetrahedra and the ZrO_6 octahedra[12].

It is well known that zirconium and hafnium ions resemble each other in chemical properties, and the two elements have nearly the same ionic radius (Zr^{4+} 86 pm and Hf^{4+} 85 pm). However, the atomic mass of hafnium is about twice heavier than that of zirconium and this is expected that the large difference in atomic mass leads to different lattice vibrations between ZrW_2O_8 and HfW_2O_8.

Raman spectroscopic study shows that $Zr_{1-x}Hf_xW_2O_8$, α-ZrW_2O_8 and α-HfW_2O_8 have a similar phonon band structures due to their structural similarity, but the replacement of Zr by Hf atoms has obvious effects on the band positions and the distribution in phonon density of states. With the contents of Hf^{4+} increasing, the internal vibrational Raman modes shift to higher, and gradually approach the mode positions of α-HfW_2O_8. The lowest asymmetric stretching modes (735 and 792 cm^{-1}) are pushed much more to higher energies than the symmetric stretching modes while the bending vibrations remain almost unchanged, resulting in a larger phonon band gap and hardening of the modes in α-HfW_2O_8.

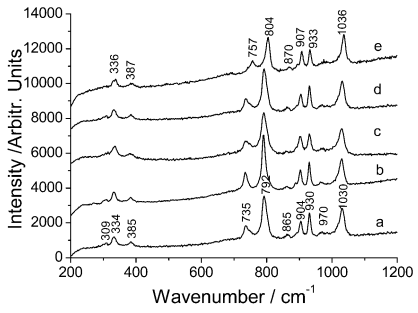

Fig. 2. Raman spectra of $Zr_{1-x}Hf_xW_2O_8$:(a) x=0, (b)x=0.1, (c)x=0.3, (d)x=0.7, (e) x=0.9.

Fig. 3 and 4 show the different temperature of the Raman spectra of $Zr_{0.7}Hf_{0.3}W_2O_8$ and $Zr_{0.3}Hf_{0.7}W_2O_8$. Only 14 modes of $Zr_{0.7}Hf_{0.3}W_2O_8$ and $Zr_{0.3}Hf_{0.7}W_2O_8$ could be

distinctly observed as compared with the predicted 54 modes at ambient temperature. As expected, the Raman spectra of $Zr_{0.7}Hf_{0.3}W_2O_8$ and $Zr_{0.3}Hf_{0.7}W_2O_8$ exhibit similar temperature behavior. With the temperature increasing, the Raman band at about 43cm^{-1} (42cm^{-1} in $Zr_{0.3}Hf_{0.7}W_2O_8$), 736cm^{-1} (737cm^{-1} in $Zr_{0.3}Hf_{0.7}W_2O_8$) become weak gradually and vanishes when the temperature is increased to 448K ($Zr_{0.7}Hf_{0.3}W_2O_8$) and 462K($Zr_{0.3}Hf_{0.7}W_2O_8$). It is well known that the entropy of α-to-β structural phase transition in ZrW_2O_8 and HfW_2O_8 is about 440K and 468 K respectively at atmospheric pressure. Above it, they undergoes a structural phase transition from an acentric (α-phase, $P2_13$) to a centric structure (β-phase, Pa_3) with increasing temperature. This indicates that a phase transition from α-to-β phase in $Zr_{0.7}Hf_{0.3}W_2O_8$ and $Zr_{0.3}Hf_{0.7}W_2O_8$ occurs about 448K and 462K approximately in accordance with its phase transition temperature reported by Toshihide Tsuji et al [13]. It can be inferred α-to-β phase transition temperature of $Zr_{1-x}Hf_xW_2O_8$ is between that of ZrW_2O_8 and HfW_2O_8 and with the contents of Hf^{4+} increasing, the phase transition temperature will increase, and gradually approach that of α-HfW_2O_8. From the facts, it can be concluded that the increase in phase transition temperature is two-fold: (i): A steady decrease in lattice parameters of $Zr_{1-x}Hf_xW_2O_8$ with increasing hafnium content. As a smaller lattice free volume makes it more difficult for the polyhedra to undergo the ratchet motion, a higher phase transition temperature is necessary. (ii): The bond strength of the Zr–O and Hf–O bonds in the solid solutions structures. Since all the $Zr_{1-x}Hf_xW_2O_8$ solid solutions has the same crystal structure as ZrW_2O_8, the phase transition mechanism of these materials are close to have the same systems. It is generally known that the mechanism of the phase transition is involved the breaking of all the metal–oxygen bonds. So it's important to compare with the bond strength of the Zr–O and Hf–O bonds in the solid solutions structures. The stronger the bonds, the higher the phase transition temperature. Since the strength of the Hf–O bond (801.77kJ/mol) is higher than that of Zr–O bond (776.18 kJ/mol), it is expected that the phase transition temperature of the solid solutions will be high with the contents of Hf^{4+} increasing.

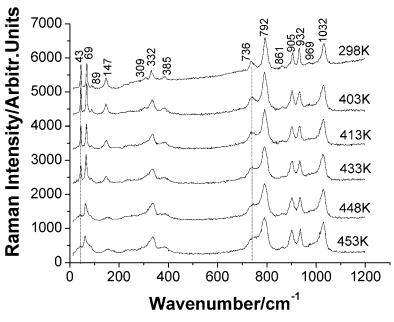

Fig. 3. Raman spectra of $Zr_{0.7}Hf_{0.3}W_2O_8$ at different temperatures.

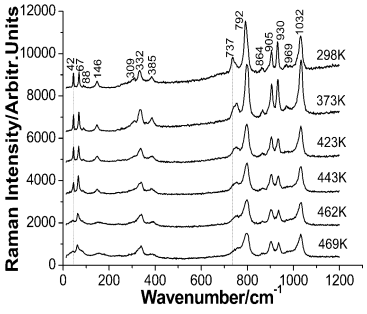

Fig. 4. Raman spectra of $Zr_{0.3}Hf_{0.7}W_2O_8$ at different temperatures.

Within the quasi-harmonic approximation, the linear thermal expansion coefficient $\alpha_V(T)$ is related to Grüneisen parameters $\gamma(T)$ as $\alpha_V(T) = \gamma(T)\frac{C_V(T)}{K_T V}$, where C_V is the isochoric specific heat, K_T is isothermal bulk modulus and V is the volume. Considering 3 N oscillators of all vibrational modes at a given temperature, the Grüneisen function $\gamma(T)$ can be written in terms of the Grüneisen parameters as $\gamma(T) = \frac{\sum_{i=1}^{3N}\gamma_i C_i(T)}{\sum_{i=1}^{3N} C_i(T)}$. From this function, a positive and negative mode Grüneisen parameter γ_i, which can be written as $\gamma_i = -(\frac{d\ln\nu_i}{d\ln V})_T$, contributes positively or negatively to the thermal expansion coefficient.

It can be seen from Figs. 3 and 4 that all of the Raman modes persist across the order-disorder phase transition, the lowest Raman mode at about 43cm^{-1} in $Zr_{0.7}Hf_{0.3}W_2O_8$ (42cm^{-1} in $Zr_{0.3}Hf_{0.7}W_2O_8$) vanishes accompanied by obvious weakening of the lowest asymmetric stretching mode (736cm^{-1} in $Zr_{0.7}Hf_{0.3}W_2O_8$ and 737 cm^{-1} in $Zr_{0.3}H_{0.7}W_2O_8$). As we know the absolute value of the thermal expansion coefficient of α-ZrW_2O_8 is larger than that of β-ZrW_2O_8. This presents direct evidence of reduction in the number of the RUMs in the high-temperature phase, which cause a smaller negative thermal expansion of the β phase. Therefore, the lowest phonon modes at about 43cm^{-1} contribute greatly to the negative thermal expansion of cubic ZrW_2O_8 and HfW_2O_8, which implying those modes have negative mode Grüneisen parameters since ZrW_2O_8 and HfW_2O_8 have negative thermal expansion coefficients. As can be seen from Figs. 3 and 4, some of the high-frequency stretching modes, particularly the asymmetric stretching modes at about 735cm^{-1} in $Zr_{0.7}H_{0.3}W_2O_8$ (736 cm^{-1} in $Zr_{0.3}H_{0.7}W_2O_8$) contribute also to the negative thermal expansion. This confirms that not only the librational motion of the WO_4

tetrahedra and the ZrO_6/HfO_6 octahedra but also the correlated motions of transilation and libration with the asymmetric stretching vibrations of the polyhedra are responsible for the negative thermal expansion in the low-temperature phase.

4. Conclusion

Powder XRD and Raman spectroscopics studies on $Zr_{1-x}Hf_xW_2O_8$ solid solutions have shown that substitution of Zr^{4+} by Hf^{4+} in ZrW_2O_8 alter the properties of ZrW_2O_8 such as cell parameters, order-disorder phase transformation temperatures and thermal stability. Lattice parameters of $Zr_{1-x}Hf_xW_2O_8$ decreased with Hf content, due to smaller ionic radius of Hf^{4+} than Zr^{4+}. $Zr_{1-x}Hf_xW_2O_8$ solid solutions and ZrW_2O_8 have the same order–disorder phase transition mechanism. The phase transition temperature will increase with increasing the content of Hf. Raman spectroscopics analyses reveal that one of the low energy modes at about 43 cm^{-1} frequency mode causes the negative thermal expansion in $Zr_{1-x}Hf_xW_2O_8$ solid solutions. In contrast to earlier belief, that asymmetric stretching modes at about 735cm^{-1} also contribute to the negative thermal expansion.

Acknowledgements

The authors acknowledge the financial support from the National Science Foundation of China (No.60876014), and the National Science Foundation of Henan province (No.132300410085).

References

[1] T. A. Mary, J. S. O. Evans, T. Vogt, A. W. Sleight, Science, **272**, 90 (1996).
[2] J. S. O. Evans, Z. Hu, et al, Science, **275**, 61 (1997).
[3] T. R. Ravindran, A. K. Arora, T. A. Mary, J. Phys. Condens. Matter, **13**, 11573 (2001).
[4] J. S. O. Evans, W. I. F. David, et al. Acta Cryst., **B55**, 333 (1999).
[5] C. A. Perottoni, J. A. H. da Jornada, Science, **280**, 886 (1998).
[6] T. R. Ravindran, A. K. Arora, T. A. Mary, J. Phys. Condens. Matter, **13**, 11573 (2001).
[7] E. J. Liang, Recent Patents on Materials Science, **3**, 106 (2010).
[8] W. Miller, C. W. Smith, D. S. Mackenzie, Mater. Sci., **44**, 5441 (2009).
[9] A. K. A. Pryde, K. D. Hammonds, et al. J. Phys. Condens. Matter , **8**, 10973 (1996).
[10] A. K. A. Pryde, M. T. Dove, et al. J. Phys. Condens. Matter , **10**, 8417 (1998).
[11] G. Ernst, C. Broholm, et al. J. Nature, **396**, 147 (1998).
[12] J. S. O. Evans, T. A. Mary, et al. Chem. Mater, **8**, 2809 (1996).
[13] T. Tsuji, Y. Yamamura, N. Nakajima, Thermochim. Acta, **416**, 93 (2004).

*Corresponding author: gxyson@126.com